Manuscript submitted to: Volume 2, Issue 2, 36-57.

AIMS Biophysics DOI: 10.3934/biophy.2015.2.36

Received date 2 January 2015, Accepted date 19 March 2015, Published date 29 March 2015

Review

Structure and Assembly of the PI3K-like Protein Kinases (PIKKs) Revealed by Electron Microscopy

Angel Rivera-Calzada [1], Andrés López-Perrote [1], Roberto Melero [1], Jasminka Boskovic [2], Hugo Muñoz-Hernández [1], Fabrizio Martino [1] and Oscar Llorca [1,*]

[1] Centro de Investigaciones Biológicas (CIB), Consejo Superior de Investigaciones Científicas (Spanish National Research Council), (CSIC); Ramiro de Maeztu 9, 28040 Madrid, Spain

[2] Electron Microscopy Unit. Structural Biology and Biocomputing Programme, Spanish National Cancer Research Centre (CNIO), Melchor Fdez. Almagro, 3, Madrid 28029, Spain

* **Correspondence:** Email: ollorca@cib.csic.es; Tel: +34-91-8373112-x4446; Fax: +34-91-5360432.

Abstract: The phosphatidylinositol 3-kinase-like kinases (PIKKs) are large serine-threonine protein kinases with a catalytic domain homologous to the phosphatidylinositol 3-kinase (PI3K). All PIKK family members share a general organization comprising a conserved C-terminus that contains the PI3K domain, which is preceded by a large N-terminal region made of helical HEAT repeats. In humans, the PIKK family includes six members, which play essential roles in various processes including DNA repair and DNA damage signalling (ATM, ATR, DNA-PKcs), control of cell growth (mTOR), nonsense-mediated mRNA decay (SMG1) and transcriptional regulation (TRRAP). High-resolution structural information is limited due to the large size (approx. 280–470 kDa) and structural complexity of these kinases. Adding further complexity, PIKKs work as part of larger assemblies with accessory subunits. These complexes are dynamic in composition and protein-protein and protein-DNA interactions regulate the kinase activity and functions of PIKKs. Moreover, recent findings have shown that the maturation and correct assembly of the PIKKs require a large chaperon machinery, containing RuvBL1 and RuvBL2 ATPases and the HSP90 chaperon. Single-particle electron microscopy (EM) is making key contributions to our understanding of the architecture of PIKKs and their complex regulation. This review summarizes the findings on the structure of these kinases, focusing mainly on medium-low resolution structures of several PIKKs obtained using EM, combined with X-ray crystallography of DNA-PKcs and mTOR. In addition, EM studies on higher-order complexes have revealed some of the mechanisms regulating the PIKKs, which will also be addressed. The model that emerges is that PIKKs, through their extensive interacting surfaces, integrate the information provided by multiple accessory subunits and nucleic acids to regulate their kinase activity in response to diverse stimuli.

Keywords: ATM; ATR; DNA-PKcs; mTOR; SMG1; TRRAP; PIKK; RuvBL1; RuvBL2; R2TP; 3D-electron microscopy

1. PIKKs, a family of large kinases that assemble higher-order complexes

Phosphatidylinositol 3-kinase-like kinases (PIKKs) are a family of large signalling proteins containing a catalytic domain with homology to the phosphatidylinositol (PI) 3-kinase (PI3K). The literature on this family of kinases is abundant, and this review discusses the cumulative findings regarding structural aspects of human PIKKs, with occasional references to some studies in yeast [1,2,3]. In mammals, the PIKK family of serine/threonine kinases comprises six members that regulate a variety of cellular processes. ATM (ataxia-telangiectasia mutated), ATR (ATM and Rad3 related) and DNA-PKcs (DNA-dependent protein kinase catalytic subunit) participate in signal transduction pathways during DNA repair and genome maintenance; mTOR (mammalian Target of Rapamycin) coordinates cell growth, proliferation and protein synthesis with the availability of nutrients and signals from growth factors; SMG1 (human suppressor of morphogenesis in genitalia 1) controls a RNA surveillance pathway known as nonsense-mediated mRNA decay (NMD); and finally TRRAP (transformation/transcription domain associated protein), the only catalytically inactive PIKK member, forms part of several complexes with histone acetylase transferase (HAT) activity. Alterations in the functions of several PIKKs are linked to a variety of diseases, reflecting their important role in human health. Some mutations in ATM and DNA-PKcs lead to ataxia-telangiectasia and severe combined immunodeficiency respectively [4,5]. These two proteins, together with ATR, are key factors in the DNA-damage response, increasing genomic instability when deregulated. As a result ATM, ATR and DNA-PKcs are attractive targets for increasing the sensitivity of cancer cells to anti-cancer therapies and to help preventing or overcoming the development of resistance [6]. In addition, mutations in SMG1 predispose to a range of cancers and mTOR signaling participates in several aspects of tumorigenesis [7,8]. It is also worth mentioning that the PIKKs involved in DNA repair seem to have also a general role in stress response signaling [9,10,11].

At the protein level, the members of the PIKK family share a common structural architecture consisting of a conserved C-terminus that contains three regions, the FAT (FRAP, ATM and TRRAP), PI3K and FATC (FAT C-terminal) domains (Figure 1) [12,13], preceded by a long stretch of helical repeats, mostly HEAT (huntington, elongation factor 3, A subunit of PP2A and TOR1) repeats [14,15]. The PIKKs have been localized to different membrane regions [16,17,18]. Localization of PIKKs to specific membrane patches is probably regulated through the many interactions these kinases are involved in, enabling different and/or locally specific signaling outputs [18,19]. The N-terminal region, made of HEAT repeats, forms a helical scaffold that is involved in protein-protein interactions, and its expanse varies considerable within the family. Nevertheless, two broad subgroups of PIKKs can be defined according to the size of their N-terminal regions (Figure 1). ATM, ATR and mTOR have molecular weights in the 280–350 kDa range, whereas DNA-PKcs and TRRAP exceed 430 kDa. SMG1 fits into the first subgroup according to the size of its N-terminal helical regions, but it contains also a unique and long insertion between the catalytic and FATC domains, of unknown function, and consequently SMG1 molecular weight reaches 410 kDa [20]. In addition, in some but not all PIKKs, such as mTOR, DNA-PKcs, TRRAP

and SMG1, a 100-residue FKBP12-rapamycin-binding (FRB) domain has been defined as a segment placed between the FAT and PI3K domains [21].

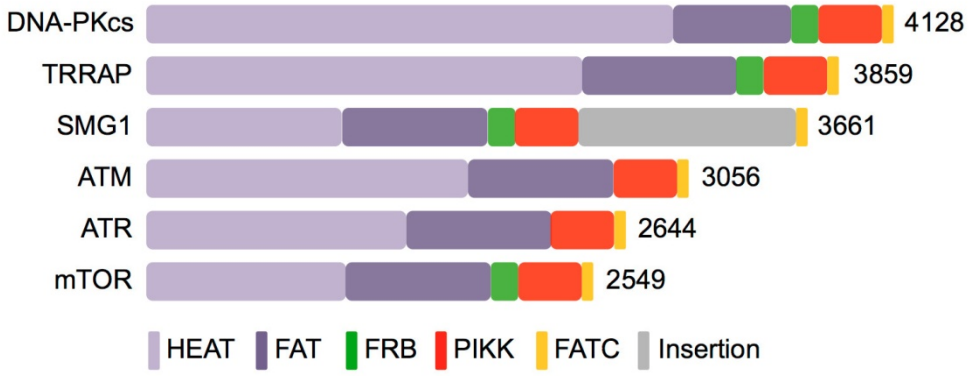

Figure 1. The PIKK family. Graphical representation of the domain organization and the total number of residues for each PIKK family member in humans.

At the cellular level, PIKKs have diverse biological functions. As previously mentioned, three PIKKs, DNA-PKcs, ATM and ATR, are implicated in double strand (ds) DNA repair [22]. DNA double-strand breaks (DSBs) are a major threat for cell viability, and they are repaired by two major pathways, homologous recombination (HR) and non-homologous end-joining (NHEJ) [23]. During NHEJ, DSBs are recognized by an abundant heterodimer of the homologous Ku70 and Ku80 proteins. Ku70/Ku80 binds to DNA ends and recruits DNA-PKcs to form a high molecular weight complex that works as a scaffold for other proteins needed for repairing the lesion [24]. The DNA-PKcs/Ku70/Ku80 complex assembled on a DNA molecule can dimerize, contributing to hold together the two ends of the DNA in preparation for joining [24,25]. Further, ATM and ATR play key roles in DNA damage signalling, and they are recruited to the sites of the DNA break through the recognition of other proteins, the MRE11–RAD50–NBS1 (MRN) complex in the case of ATM and the ATRIP protein in the case of ATR [26,27].

mTOR is a nutrient-regulated protein that controls a wide variety of pathways involved in metabolism and cell growth, and it has been proposed as a target for the development of new anti-cancer drugs. In 1991 two genes, *TOR1* and *TOR2*, were identified in yeast using genetic screens that looked for mutations that rescued the anti-proliferative effect of rapamycin (TOR stands for target of rapamycin) [28]. However, mammals contain a single copy of the TOR gene, mTOR, which associates as part of two distinctive multi-protein complexes, mTORC1 and mTORC2 [29]. mTORC1 integrates information from growth factors, hormones, nutrients and energy signals to regulate cell growth by phosphorylating regulators of translation, S6K1 and 4E-BP1, and thus stimulating protein synthesis. On the other hand, mTORC2 is one of the kinases responsible for the phosphorylation of the hydrophobic motif of Akt/PKB, required for full stimulation of Akt/PKB activity. mTORC2 also plays a role for cytoskeletal rearrangements and cell survival, and also for some metabolic issues [29,30].

SMG1 plays a critical role in nonsense-mediated mRNA decay (NMD), a surveillance pathway that degrades mRNAs containing premature termination codons [31]. NMD discriminates correct and

aberrant translation termination events and SMG1-mediated phosphorylation of the RNA helicase UPF1 is believed to be an essential step to trigger the NMD response. The kinase activity of SMG1 is regulated by a sophisticated, and incompletely understood, interplay of protein-protein interactions. Two factors, SMG8 and SMG9, form a tight complex with SMG1, the so-called SMG1C (SMG1 Complex), that it is thought to down-regulate SMG1 kinase [32]. On the other hand, the association between SMG1 and UPF1 with other proteins, such as UPF2, UPF3 and the exon-junction complex (EJC), seems to be required to induce SMG1-mediated UPF1 phosphorylation [33,34].

Finally, TRRAP is the only member of the PIKK family that has lost its catalytic function as a kinase, and it seems to have specialized as a scaffold for the assembly of several large macromolecular complexes, mainly implicated in the remodelling of chromatin, which is an important step for the transcriptional activity of several transcription factors [35,36].

2. Advantages of single-particle electron microscopy to study PIKKs

Full molecular understanding of the mechanisms that regulate PIKK function needs structural models for these kinases and their complexes. Despite their relevance in key cellular processes, high-resolution structural information is scarce, limited to the mTOR and DNA-PKcs structures [21,37]. Apart from their large size and complex architecture some of the complexes are difficult to purify in amounts necessary for X-ray crystallography structural studies. The anticipated conformational heterogeneity of these complexes in response to phosphorylation, DNA and protein binding, and the heterogeneity in the composition of some of these complexes add further challenges to their structural characterization.

Electron microscopy (EM) has benefits as requiring modest amounts of material for observation in the microscope and the use of mild fixation can help to stabilise transient and low affinity interactions [38]. Moreover, single-particle EM has the potential to address conformational and compositional heterogeneity of the PIKKs [39,40]. These facts have turned single-particle EM into a major source of structural information for PIKKs and their complexes, together with X-ray crystallography, NMR and SAXS studies of these kinases [21,25,37,41,42]. Although cryo-electron microscopy (cryoEM) has been applied to mTOR and DNA-PKcs complexes [43,44,45], negative stain EM remains a source of significant information about the core structural features of these kinases. Sample preparation using negative staining can be a good choice when the amount of sample is very limited, and the structural information obtained using this technique can still be useful [40]. Nevertheless interpretations of this data beyond what is reasonable for the details and resolution reached in each case should be avoided. Currently the resolution of the EM studies on PIKKs are in the ~20 Å range as the available EM studies on these kinases have been performed before the spread of the use of direct electron detectors [46]. The use of these new technologies in the study of the PIKKs will surely reveal new and exciting insights in their structure and regulation.

3. Structural model of the PIKK family based on EM structures

Single-particle EM has been especially successful in visualising several members of the PIKK family obtaining structures for human ATM, DNA-PKcs and SMG1, as well as TOR from *Saccharomyces cerevisiae* at intermediate resolutions [39,40,47,48,49]. ATM, DNA-PKcs, SMG1 and TOR have been studied using negative staining, mostly due to the low yield of protein purified

after expression in yeast, human or mammalian cells. CryoEM imaging has also been applied to SMG1, mTOR and DNA-PKcs but only in the last case sub-nanometer resolution has been reached [43,44,45,48]. These studies on human DNA-PKcs and SMG1 together with the atomic structure of a C-terminal fragment of mTOR and the atomic model of human DNA-PKcs [21,37] have been particularly relevant to provide structural information that can be integrated into an architectural model of the PIKK family, and thus, these are discussed in more detail below.

Several groups have extensively studied the structure of human full-length DNA-PKcs and this was the first PIKK protein analyzed by cryoEM [50]. A year later Leuther K. K. and colleagues published the structure of human full-length DNA-PKcs at 20–30 Å solved from negatively stained two-dimensional (2D) crystals [51] (Figure 2A). This structure clearly revealed that DNA-PKcs was organized in two main structural regions, the head and the arm/arms. Part of these arms formed an intricate region at the opposite end of the head, which was named the "palm" by some authors [39]. A similar overall organization of DNA-PKcs was observed in all of the subsequent structures of DNA-PKcs solved by EM [24,39,44,45] (Figure 2B–2C). A combination of antibody labeling and EM as well as the fitting of the crystal structures of a PI3K and segments of HEAT repeats into a cryoEM structure of DNA-PKcs strongly suggested that the head of these structures comprised the C-terminal region of DNA-PKcs whereas the arms contained the N-terminal HEAT repeats [45]. Subsequently a cryoEM structure of DNA-PKcs at 7 Å resolution confirmed the presence of alpha helical elements in the arms, further reinforcing this model [44].

The overall structure of DNA-PKcs was conclusively outlined with the crystal structure of DNA-PKcs at 6.6 Å resolution that was obtained in complex with the C-terminal domain of Ku80, although density for this interacting partner was not identified in the map [37] (Figure 2D–2E). In this structure, helical regions were clearly visible in the electron density and although the authors were not able to trace the polypeptide chain, the data definitely confirmed that the head region contained the kinase domain. This assignment correlates well with the atomic structure of a C-terminal fragment of mTOR [21]. Interestingly the N-terminal end of DNA-PKcs was found forming two arms projecting from the head and creating an open circular structure, although the resolution did not permit to discard other possible interpretations (Figure 2D–2E). Thus some uncertainties remained, such as how the two arms were connected and how to relate specific segments of the sequence with the structure. Interestingly, EM structures of DNA-PKcs obtained using negative staining, but also several cryoEM structures, suggested that the organization of the arm region was apparently more complex, and sub-regions such as "palm" or "insertion" were defined based on these low resolution EM structures [39,44,45,51] (Figure 2A–2C). This more elaborate architecture of the arm region was also evident in projection images of DNA-PKcs 2D crystals, suggesting that these were real structural features [51].

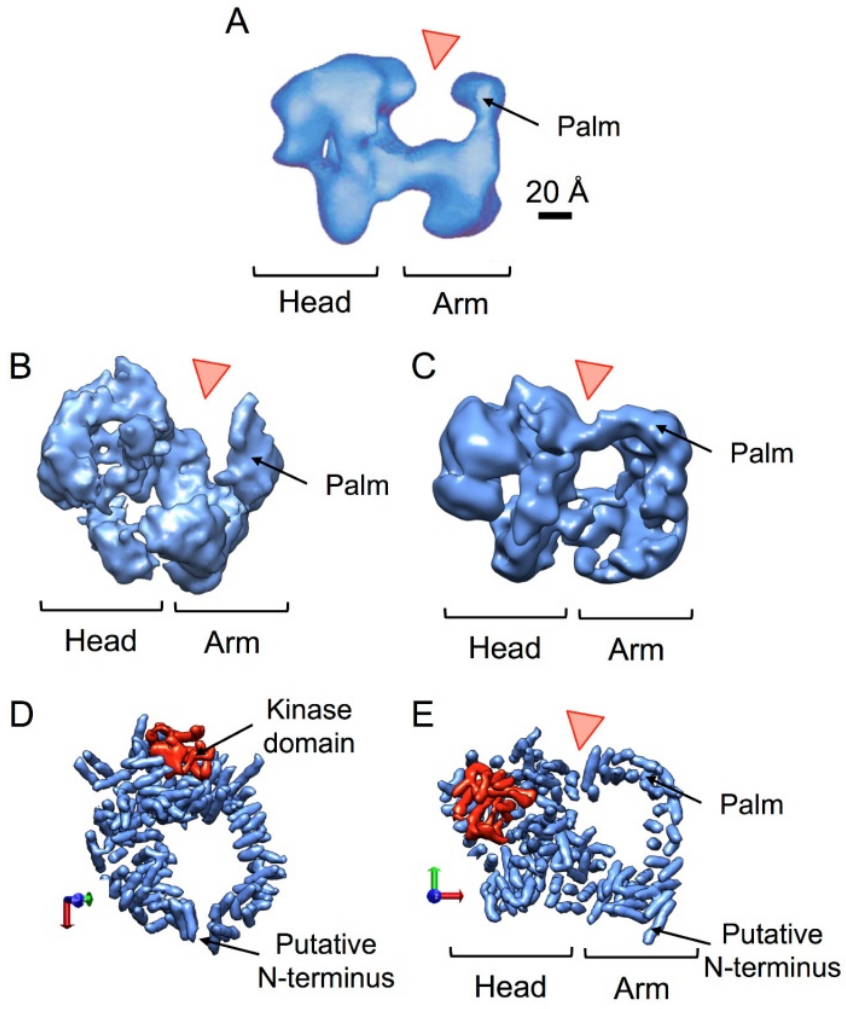

Figure 2. The structure of DNA-PKcs. (A) 3D structure of DNA-PKcs at 22 Å resolution obtained from 2D crystals [51], defining two structural regions, head and arm. A sub-region in the arm was named palm. A discontinuity in the arm region is indicated with a red triangle. The scale bar corresponds to 20 Å, and is compatible with the rest of the panels. Adapted from [51] according to Copyright Clearance Center's (CCC) terms and conditions. (B) and (C) CryoEM structures of DNA-PKcs, (EMD-1102) [45] (B), and EMD-5831 [44,65] (C), indicating the head and arm regions. (D) and (E) Two views of the crystal structure of DNA-PKcs shown after being filtered to an approximate resolution of 8 Å (PDB ID: 3KGV) [37]. The catalytic domain is coloured in red. The putative position of the N-terminus is indicated. In (E) the structure is shown in an orientation compatible with those in panels (A), (B) and (C).

A possible reconciliation of all these studies could come from the analysis of different views of the molecules. Some orientations of the crystal structure of DNA-PKcs obtained after rotating the molecule are comparable to the structures obtained by EM (Figure 2). Although the EM structures suggest a discontinuity in the arm region (Figure 2A–2C, labeled with a red triangle) that is not clearly observed in the crystal structure (Figure 2E), the overall structural organization is similar. The

conformational flexibility of the arms could in addition account for some of the discrepancies between the structures solved. HEAT repeat domains of several proteins change their conformation dramatically upon ligand binding [52,53]. In DNA-PKcs, conformational changes in the N-terminal regions occur after DNA binding and after phosphorylation, as shown by EM and SAXS [25,39]. Thus it is conceivable that differences between the several EM structures solved reflect this conformational flexibility. It can also not be ruled out that some of the EM reconstructions reported were partially incorrect by reflecting the average of an undefined mixture of conformations in these flexible domains. Image classification and computational sorting could potentially address this conformational heterogeneity, but this is still a challenging task, and such flexibility could have passed unnoticed at the time these structures were solved.

The structural organization of PIKKs has been further clarified by the recent 3D structure of SMG1 at 22 Å resolution [40,48]. The resolution of this structure was sufficient to unambiguously identify the head domain and the HEAT repeat region. The crystal structure of the C-terminus of mTOR fitted the overall shape of the head very convincingly, allowing the identification of several domains (Figure 3A). According to that model, the FRB domain appeared in SMG1 as a protrusion from the globular head, and interestingly this domain has been proposed to regulate the access of substrates to the catalytic domain in mTOR [21]. SMG1 reveals only one arm whose conformation is similar to one of the arms of DNA-PKcs [40]. This suggests that the N-terminal HEAT repeat region of SMG1, together with the other "small" PIKKs (ATM, ATR and mTOR), probably comprises just one helical "arm", whereas DNA-PKcs and possibly TRRAP would have acquired a second "arm" to accommodate some of their specific functions, such as the interaction with DNA repair factors in the case of DNA-PKcs (see below). This model is supported by the low-resolution EM structures of human ATM [47] (Figure 3B) and *S. cerevisiae* TOR [49] (not shown), which revealed only one twisted arm protruding from the head and by predictions of the structure of the N-terminal region of mTOR [54]. Further supporting this model, projection EM images of Tra1, yeast homolog of TRRAP, as part of a larger complex, are similar to those of DNA-PKcs (see below).

Summarizing the above, work on several PIKKs by EM and X-ray crystallography has provided a convincing picture of the mayor structural features of the PIKK family. The conserved C-terminus forms a compact region, named "head" at low resolution, and a crystal structure of this region in mTOR has revealed in atomic detail how these conserved domains are organized [21] (Figure 3C). This crystal structure revealed that access to the active site is restricted by the FRB domain [21]. Thus, the specific recruitment of substrates to the kinase domain could be an important mechanism to regulate mTOR, and maybe other PIKKs. The long N-terminal regions assemble as helical scaffolds typical of HEAT repeats. These can change conformation dramatically after protein/DNA binding or phosphorylation (see below). These structures left several issues unresolved. The crystal structure of mTOR is missing parts of the FAT domain, and thus, the structural details on how the C-terminal region is preceded by the N-terminal helical repeats is missing [21]. Also the structure and organization of the C-terminal insertion in SMG1, or the structure of the whole C-terminus in ATM and ATR that probably lack an FRB domain [21], are not known. As a consequence we do not completely understand what is the organizing principle that distinguishes the 250 kDa from the 420 kDa PIKKs.

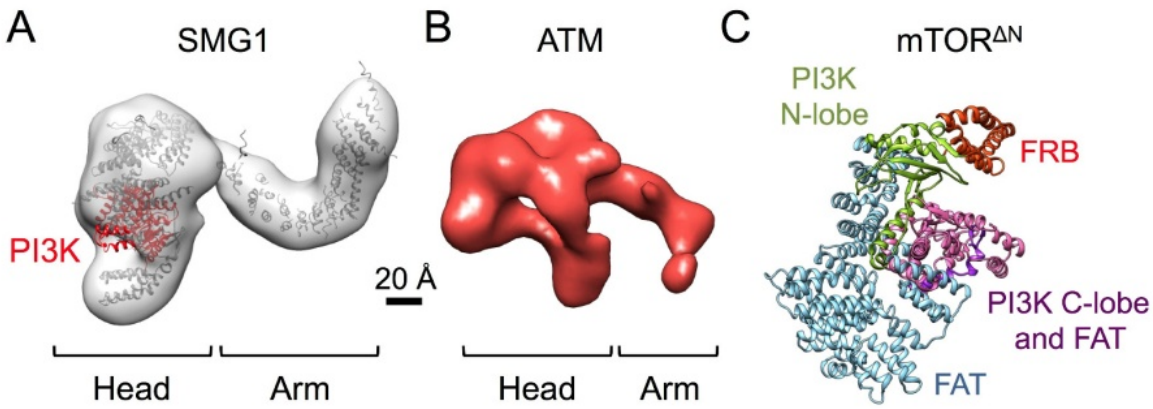

Figure 3. EM structures of SMG1 and ATM, and crystal structure of mTOR C-terminus. (A) EM structure of SMG1 (EMD-2662) [40] fitted with the crystal structure of mTOR C-terminal region (PDB ID: 4JSV) [21] (head region) and a segment of HEAT repeats from DNA-PKcs (PDB accession code 3KGV) [37] (arm region). The catalytic domain (PI3K) is shown in red. (B) EM structure of ATM [47]. In (A) and (B) the head and arm regions are indicated, and the scale bar corresponds to 20 Å (C) Ribbon representation of the crystal structure of mTOR C-terminus (PDB accession code 4JSV) [21] with the characteristic domains indicated and colored differently. The two lobes of the kinase domain are also highlighted.

4. Several PIKKs dimerise to control their activation

Several PIKKs have been described to form dimers. Interestingly, in some cases dimerization appears to be a major controller of protein activation. A few dimers were found in electron micrographs of purified DNA-PKcs [39], but a significant number of dimeric complexes were observed in preparations of the DNA-PK holo-enzyme, comprising a complex between DNA-PKcs and Ku70/Ku80, bound to a short DNA fragment [24,55] (Figure 4A, panel i). These dimeric complexes were proposed to be structural intermediates in the DNA repair reaction, by forming a synapse maintaining the broken DNA ends in proximity, while allowing the various enzymes required to complete the repair reaction to access the lesion [23]. The conformation of these DNA-PK dimers can be affected by several factors (see below), as observed both by EM and SAXS [25,56] (Figure 4A, panels ii and iii).

Probably one of the most intriguing dimerization processes in the PIKK family has been described for ATM. Compelling biochemical evidence revealed that ATM can form a dimer by contacts between the kinase domain of one ATM molecule and the FAT domain of other ATM molecule, within a region surrounding serine 1981 [57]. ATM is kinase-inactive as part of this complex but ATM-mediated auto-phosphorylation of serine 1981 after DNA damage dissociates the complex and releases a phosphorylated and "activated" ATM monomer, which is now capable of phosphorylating other substrates [57]. Nevertheless, ATM can be additionally activated by oxidation through the formation of disulphide-linked dimers, which are mechanistically distinct from those involved in DNA damage activation [58,59]. Dimers of ATM have been observed in negative stained

EM samples [47], however up to our knowledge, we are still missing a structure of these ATM dimers that could provide some light into how these distinct dimerization processes regulate ATM activation.

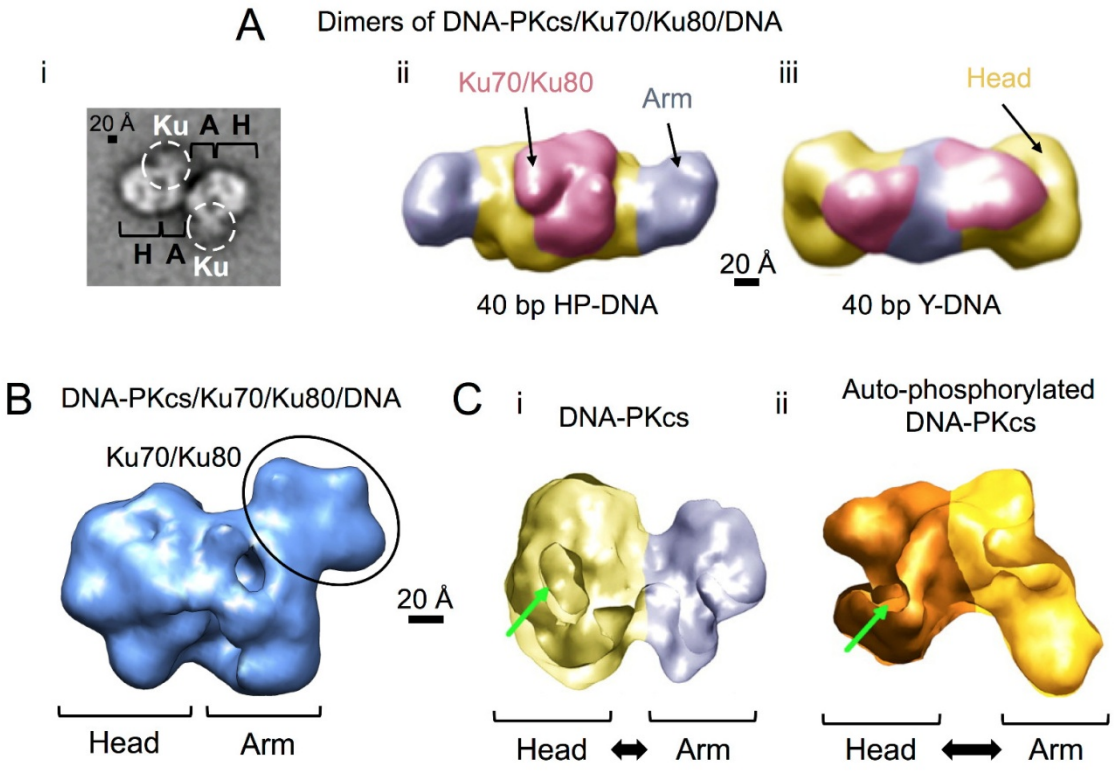

Figure 4. Dimerization and higher order complexes of DNA-PKcs. (A) Structure of dimers of DNA-PKcs/Ku70/Ku80/DNA complexes. (i) A reference-free class-average of DNA-PKcs/Ku70/Ku80/DNA dimers [24]. Scale bar represents 20 Å. The position of Ku70/Ku80 heterodimers within the complex is encircled and labelled as Ku. The characteristic head [H] and arm [A] domains in DNA-PKcs are also indicated. Two representative SAXS envelopes of DNA-PKcs/Ku70/Ku80 complexes assembled on a 40 base pair (bp) dsDNA either with a hairpin (HP-DNA) (ii), or a Y-shaped DNA structure at one end (Y-DNA) (ii) [25]. The Ku70/Ku80 molecule and the head and arm regions in DNA-PKcs are indicated. For (ii) and (iii) the scale bar corresponds to 20 Å. (B) One view of a negative-stain EM structure of the DNA-PKcs/Ku70/Ku80/DNA complex (EMD-1209) [24]. Density corresponding to the Ku70/Ku80 heterodimer is shown encircled. (C) Auto-phosphorylation of DNA-PKcs causes a large conformational change that correlates with the opening of the structure [25]. Cut-open SAXS envelopes for DNA-PKcs (i) and auto-phosphorylated DNA-PKcs (ii). A green arrow indicates the characteristic cavity in the head region and a black arrow highlights the increased distance between head and arm after phosphorylation. For (B) and (C) the scale bar corresponds to 20 Å. Panels shown in (ii) and (iii) in (A) and (C) have been adapted from [25] according to Creative Commons (CC)-BY license terms and conditions.

5. Higher-order complexes regulate PIKK kinase activity

PIKKs perform diverse and complex biological functions in the cells, which must be tightly regulated. PIKK activities are controlled by two principal mechanisms, the organized recruitment of the protein to those sites where needed, and by regulating (activating or restraining) its kinase activity. Thus ATM, ATR and DNA-PKcs kinases that participate in the DNA repair response are recruited to specific sites of damage by interaction with other proteins. *In vitro* and *in vivo* experiments have shown that binding of ATM to the MRN complex is required for full activation of ATM. This interaction is achieved through direct contact between specific domains in ATM and NBS1 [60]. On the other hand, during NHEJ DNA-PKcs activation is dependent on its recruitment to the sites of DNA double-strand break. This is achieved by DNA-PKcs ability to bind DNA and form a complex with Ku70/Ku80, which is first recruited to sites of damage (see below). Furthermore, SMG1, the kinase determining the fate of an aberrant mRNA, can be specifically recruited to a stalled ribosome as part of a complex containing release factors eRF1 and eRF3, and UPF1, an RNA-dependent helicase, the so-called SURF (SMG1-UPF1-eRF1-eRF3) complex [34]. But certainly the main mechanism regulating PIKKs is the control of their kinase activity on the specific targets. This is mostly achieved by formation of higher-order complexes with other proteins, and in some cases activation of the protein as part of larger complexes is coupled to the process of recruitment to the sites where PIKKs are required. In addition, in some cases, phosphorylation and binding to DNA further contribute to regulate its kinase activity. Structural information for these regulatory processes has been mostly obtained thanks to single-particle EM, and below we review the most significant findings.

DNA-PKcs is recruited to sites of double-strand breaks by Ku70/Ku80, a 150 kDa heterodimer containing a preformed ring structure capable of encircling dsDNA in a sequence-independent manner (Figure 4B). This interaction between DNA-PKcs and Ku70/Ku80 significantly stimulates its kinase activity [61]. *In vitro*, DNA-PKcs binds DNA independently of Ku70/Ku80 but with less affinity than the Ku hetero-oligomer. When part of the complex with Ku70/Ku80 DNA-PKcs also interacts with DNA [61]. An EM structure of a DNA-PKcs/DNA complex suggested that the arm regions in DNA-PKcs embrace DNA, although the low resolution of these studies did not allow defining the specific region involved in DNA recognition [39]. Potential DNA binding sites have been proposed based on a cryoEM structure of DNA-PKcs [44]. Conformational changes in the arm upon DNA binding have also been visualized for ATM, by comparing the EM structures of ATM an ATM-DNA complex resolved at low resolution using negative staining [47]. Interestingly the intermediate resolution EM structures of the human DNA-PKcs/Ku70/Ku80 complex assembled on a DNA molecule revealed that Ku70/Ku80 interacted with the arms (Figure 4B), and it was speculated that the larger N-terminal regions in DNA-PKcs could be an adaptation to interact with other factors required for NHEJ and/or the DNA [24]. Despite the low resolution of these studies, the structures of the DNA-PKcs/Ku70/Ku80/DNA complex suggested that binding of Ku70/Ku80 elicited conformational changes in the C-terminal regions of DNA-PKcs. All together, these findings indicated that conformational changes induced by Ku70/Ku80 binding and/or DNA in the HEAT region contribute to regulate the kinase activity.

This model is further supported by our current understanding of the regulatory role of DNA-PKcs auto-phosphorylation in NHEJ [56,62,63,64]. SAXS and EM studies have addressed the structural consequences of DNA-PKcs auto-phosphorylation (Figure 4C). SAXS experiments

performed using DNA-PKcs and DNA-PKcs/Ku70/Ku80/DNA complexes revealed substantial conformational changes upon auto-phosphorylation consisting mainly on a large opening of the entire DNA-PKcs molecule, at least at the low resolution of these studies [25]. EM of complexes between DNA-PKcs and Ku70/Ku80 in the presence of a short dsDNA fragment revealed that whereas the DNA-PKcs/Ku70/Ku80/DNA complex was rather homogenous before phosphorylation, auto-phosphorylation induced a considerable degree of heterogeneity in the sample as well as a major tendency to disassemble the dimeric complexes [56]. This finding suggested an extensive remodeling of the DNA-PK holoenzyme as a consequence of auto-phosphorylation, which could be important during NHEJ. Curiously, EM images of DNA-PKcs/Ku70/Ku80/DNA complexes obtained by other authors showed that Ku70/Ku80 adopted a large variability of orientations with respect to DNA-PKcs [65]. This result was interpreted as an indication of a flexible linkage between both DNA and Ku70/Ku80 to DNA-PKcs. A full understanding of the functions and regulation of DNA-PKcs during NHEJ will probably require the analysis of even larger complexes containing additional double-stranded DNA repair factors such as XRCC4, Ligase IV and XLF.

TRRAP belongs, together with DNA-PKcs, to the sub-group of PIKKs containing a larger N-terminal HEAT repeat region. Although structural information for TRRAP is scarce, EM images and structures of yeast histone acetyltransferase complexes NuA4 and SAGA, containing TRRAP-homolog Tra1, also suggested that the N-terminal regions act as a scaffold interacting with other proteins [66,67] (Figure 5A).

mTOR forms part of two complexes, mTORC1 and mTORC2, which have been extensively studied and characterized due to their relevance in human health. These are functionally distinct; while mTORC1 regulates cell growth in response to nutrients and energy in the cell, mTORC2 controls proliferation as a kinase responsible for AKT/PKB phosphorylation [29]. mTORC2 plays several other functions, such as participating in cytoskeletal rearrangements and cell survival [29,30]. Interestingly, this functional distinction between mTORC1 and mTORC2 is believed to be defined biochemically by a discrete selection of interacting partners. mTORC1 is composed of mTOR, regulatory-associated protein of mTOR (RAPTOR) and non-core components PRAS40 and DEPTOR, whereas mTORC2 is made of mTOR in complex with RICTOR [29]. Other subunits are common to both complexes, such as mammalian Lethal with SEC13 protein 8 (mLST8). Human mTORC1 complexes containing mTOR, RAPTOR, mLST8 and PRAS80 analyzed by EM revealed a large dimeric complex of rhomboid shape around a central cavity whose structural integrity can be compromised by incubation with FKBP12-rapamycin [43] (Figure 5B). How these large assemblies contribute to regulate the functions of mTORC1 and how these structures relate to the crystal structure of the mTOR fragment bound to mLST8 remains unclear. EM experiments using staining agents provided a low-resolution structure of yeast TOR in complex with RAPTOR homolog KOG1. This model suggested that the full-length protein was also organized as a “head” region connected to an “arm”, and KOG1 seemed to interact extensively with regions of both the head and the arm. However dimers were not found under their experimental conditions [49].

The recent determination of the atomic structure of a fragment of mTOR comprising several of the conserved features of the PIKK C-terminal region (see above) has been a major breakthrough in our understanding of PIKKs architecture [21]. This structure was solved in complex with mLST8, providing interesting insights on the regulation of mTOR (Figure 5C). This structure showed that the catalytic site of mTOR had an active conformation but located at the bottom of a cleft restricting the access of substrates. Also, the predicted location of RICTOR and RAPTOR in the complex could

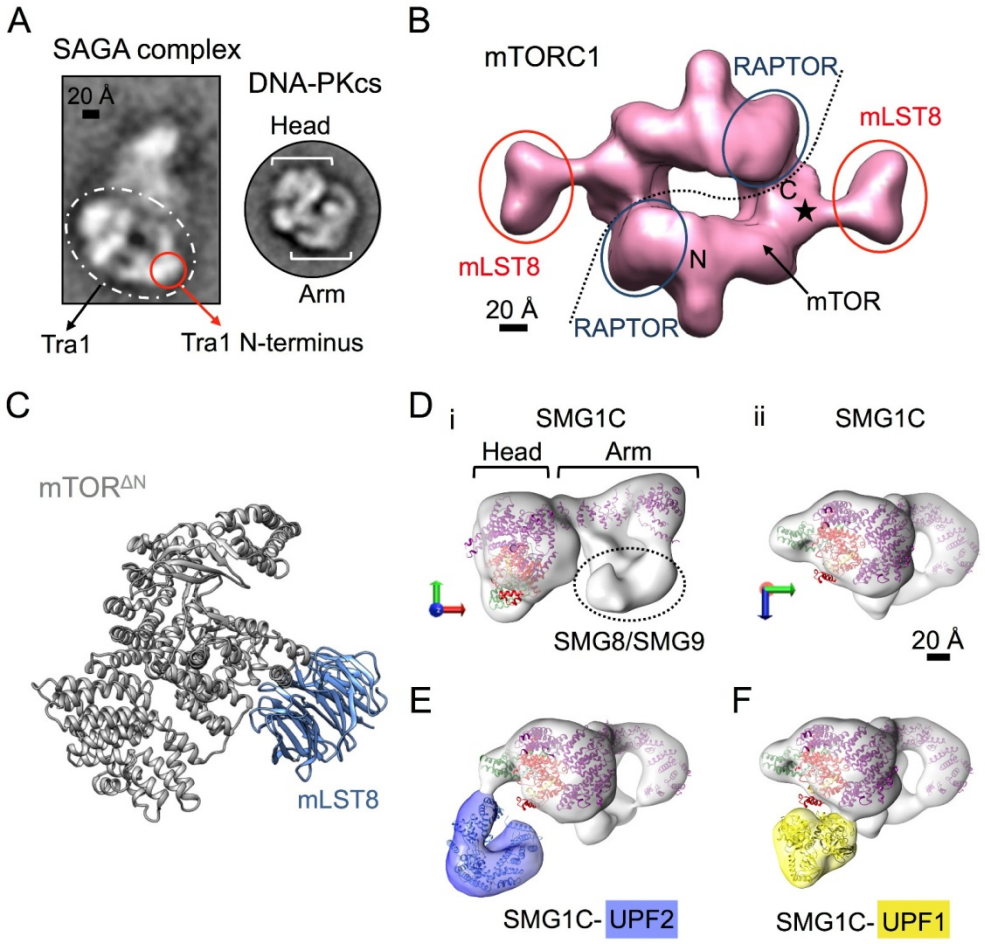

Figure 5. Higher order complexes assembled by PIKKs. (A) Comparison between representative negative stain 2D projections obtained by EM of the yeast SAGA complex and human DNA-PKcs. Density corresponding to the TRRAP-homolog Tra1 is shown encircled, and the probable location of its N-terminus is pointed [66]. Both images are shown at the same scale and the measuring bar corresponds to 20 Å. 2D projection of the SAGA complex has been adapted from [66] according to CCC terms and conditions. (B) CryoEM structure of dimeric human mTORC1 (EMD-5197) [43]. The proposed locations of the N- and C-terminal domains (labeled as N and C) and the kinase domain of mTOR (black star) are indicated. Densities assigned to RAPTOR and mLST8 are shown encircled in blue and red respectively. The dotted line represents the dimer interface. The measuring bar corresponds to 20 Å. (C) Ribbon representation of the crystal structure of the mTOR C-terminus/mLST8 complex (PDB ID: 4JSV) [21]. mTOR C-terminus is shown in grey and mLST8 in blue. (D) Negative-stain EM structure of human SMG1C. (i) and (ii), two views of the SMG1C complex, comprising SMG1, SMG8 and SMG9 (EMD-2663) [40]. The characteristic head and arm regions are shown, and the density corresponding to SMG8 and SMG9 is encircled. The density of SMG1 is fitted with the C-terminal region of mTOR crystal structure (PDB ID: 4JSV) (head region) [21], and a segment of HEAT repeats from DNA-PKcs (PDB ID:

3 KGV) [37] (arm region). The HEAT and FAT domains are shown in dark purple, the FRB domain in green and the catalytic domain in red. (E) Negative-stain EM structure of the SMG1C-UPF2 complex (EMD-2665) [40]. The density corresponding to UPF2 is shown in blue and fitted with an atomic model for the structure of UPF2. (F) Negative-stain EM structure of the SMG1C-UPF1 complex (EMD-2664) [40]. The density corresponding to UPF1 is shown in yellow and fitted with the atomic structure of the closed conformation of UPF1 (PDB ID: 2XZL) [85]. In (E) and (F) SMG1C is shown in the same orientation as in D, panel ii. The scale bar corresponds to 20 Å for the panels in (D), (E) and (F).

further contribute to restrain the accessibility of substrates to the catalytic sites. Thus, the authors proposed that substrate recruitment could be one of the main mechanisms regulating phosphorylation by mTOR. This model could be likely extended to other PIKKs since activation of ATM and SMG1 seems to be coupled to their recruitment to the sites where their targeted substrates are located [32,68]. Their model also suggested that rapamycin-FKBP12 inhibits mTOR, at least in part, by further affecting the accessibility to the catalytic site. mLST8 is thought to be required for mTOR activity and the structure showed that it binds to an insertion in the catalytic domain, which could contribute to the stability of an active conformation [21].

Additional insights into the mechanisms involved in PIKK regulation have been recently revealed by the EM structure of SMG1C [40,48] (Figure 5D, panels i and ii). SMG8 (991 amino acids) and SMG9 (520 amino acids) were found to co-purify with SMG1 forming a tight complex during purification [32,48]. The association between these two proteins and SMG1 was essential for a correct function of the NMD pathway and *in vitro* kinase assays revealed that these interactions contributed to down-regulate the kinase activity of SMG1. It was thus proposed that one of the functions of these interactions could be the control of the kinase activity of SMG1 until an aberrant mRNA was detected and NMD had to be triggered. Notably EM data revealed that the SMG8 and SMG9 interacted with SMG1 HEAT repeat region inducing a large rotation of the arm [40]. Since *in vitro* incubation of SMG8/SMG9 with SMG1 is sufficient to down regulate SMG1 kinase [48], such conformational change must be sufficient to affect its kinase activity.

The recruitment of substrates to the kinase domain has been proposed as one of the mechanisms that regulate mTOR [21], but the mechanisms taking place within the entire PIKK family are probably more complex. Full activation of SMG1 kinase on UPF1 requires further stimulus by at least another two NMD factors, UPF2 and UPF3 [33,34]. The recent EM structures of SMG1C-UPF1, SMG1C-UPF2 and SMG1C-UPF1-UPF2 have shown the architecture of these complexes, and illuminated some of the structural basis of SMG1 regulation [40] (Figures 5E–5F). The structures revealed that, in contrast to SMG8 and SMG9, both UPF1 and UPF2 bind SMG1C in the proximities to the kinase domain, with the potential to influence the conformation of the kinase domain more directly. Furthermore, these structures combined with several competition and interaction experiments showed that interactions between UPF1 and UPF2, required for the full activation of UPF1, could take place within the platform provided by SMG1C.

6. Integrated structural model for the regulation of PIKKs

Taking all the information above, the model that emerges is that PIKKs are complex platforms

containing several regions prepared for specific interactions with other proteins and DNA. Through their extensive interacting surfaces, PIKKs integrate the information provided by multiple accessory proteins and nucleic acids and modify accordingly their kinase activity to response to the diverse stimuli (Figure 6).

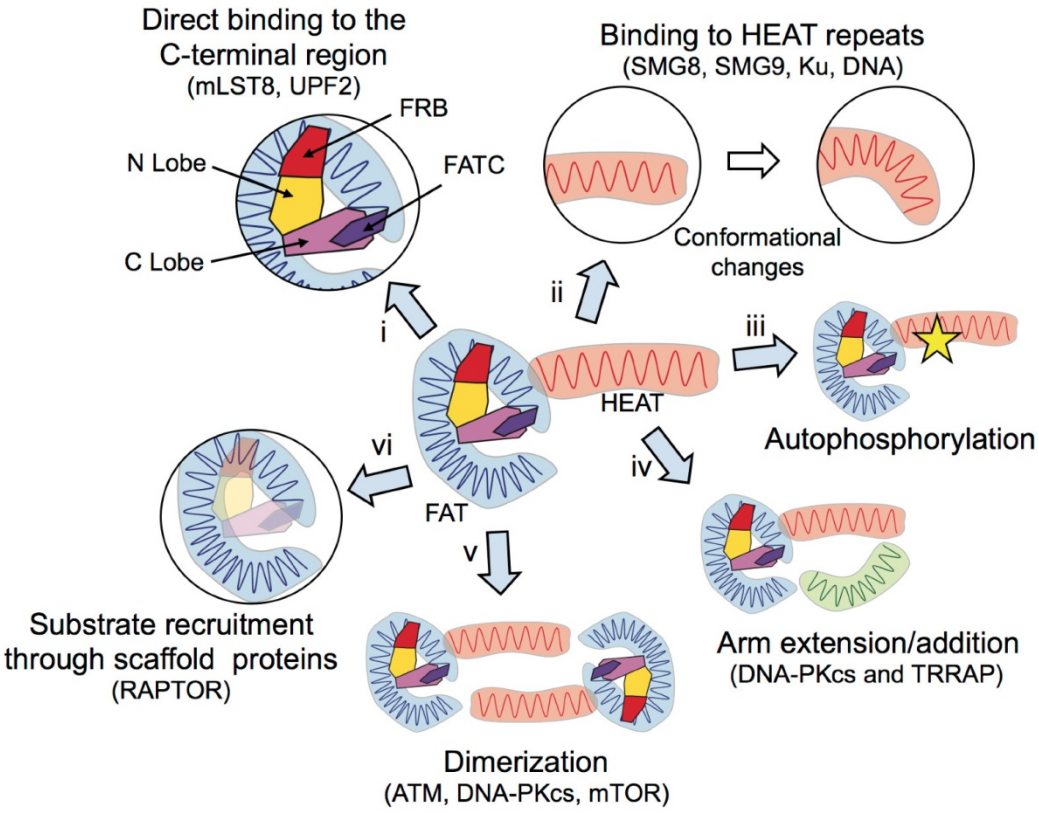

Figure 6. Structural model for the PIKK family. The central panel represents a simplified cartoon version of the topological organization for the PIKKs. The accessibility to the catalytic domain can be modulated by the FRB domain in those PIKKs in which is present. The FATC domain interacts with the activation loop in the C-lobe of the kinase domain, possibly contributing to its stabilization. This arrangement is nested by the FAT domain (in blue), and together with the catalytic domain forms the head. The FAT creates extensive interaction surfaces for the binding of additional factors, and these interacting surfaces can be extended through an additional domain made of HEAT repeats that corresponds to the arm. The structural complexity of the PIKKs correlate with their capacity to regulate complex biological processes. PIKKs can be regulated through diverse mechanisms: (i) direct binding of factors to the catalytic region (mLST8, UPF2), (ii) binding of proteins (SMG8/SMG9, Ku70/Ku80) or DNA to the HEAT repeats in the arm; (iii) autophosphorylation; (iv) addition/extension of new interacting surfaces made of HEAT repeats to recruit specific factors; (v) through homo-dimerization; (vi) and by substrate recruitment mediated by other scaffold proteins, such as RAPTOR in mTOR.

HEAT repeat regions appear to be a major player in the regulation of PIKK function. These are organized as a single twisted helical arm in ATM, ATR, SMG1 and mTOR, whereas a second arm appears in DNA-PKcs and TRRAP, probably to deal with specialized functions of these proteins. These helical scaffolds are involved in multiple protein-protein interactions in all PIKKs, and they are also involved in DNA binding. These interactions are required to recruit PIKKs to their sites of action, but they also induce conformational changes that somehow, directly or indirectly, can regulate the kinase activity. Phosphorylation of the HEAT repeat region and/or dimerization could also function to alter the conformation of the arms, regulating kinase activity indirectly or by restricting the accessibility of the kinase domain for substrates. On the other hand, several factors bind to the C-terminal regions, which directly regulate the kinase activity, but also some factors function by recruiting the substrates to the active site of the kinase. PIKKs can therefore integrate the inputs provided by all these interacting factors, through conformational changes, to either activate or restrain its kinase activity.

7. Assembly and maturation of PIKKs by the R2TP and TTT complexes

In addition to the complex regulation of PIKKs, recent research has exposed that maturation and correct assembly of several, possibly all, PIKKs requires a cooperation of sophisticated chaperon machinery. The R2TP complex was discovered in yeast as a complex containing the yeast homologs of human RuvBL1 ("RuvB-like" 1) and RuvBL2 ("RuvB-like" 2), Tah1 (Spagh/RPAP3 in humans) and Pih1 (in Pih1D1 humans) [69]. This complex has emerged as an essential factor for PIKK maturation, as well as for other large complexes such as snoRNPs and RNA polymerases [70]. R2TP binds both heat shock protein 90 (HSP90) and the PIKKs possibly acting as a HSP90 co-chaperon that brings PIKKs to the chaperon (Figure 7A). Association between PIKKs and the R2TP complex is mediated by Tel2, a protein that binds PIKKs as part of a larger TTT (Tel2-Tti1-Tti2) complex [71,72]. Tel2 is phosphorylated by casein kinase 2 (CK2) generating a specific phosphopeptide that is recognized by the R2TP complex [73]. Interestingly, some evidence about the role of RuvBL1 and RuvBL2 in NMD suggests that they do not only regulate SMG1 abundance but they also associate with SMG1 and the messenger ribonucleoproteins in the cytoplasm to promote the assembly of SMG1-containing complexes that are required as structural intermediates for an NMD response. It has not yet been addressed if RuvBL1 and RuvBL2 perform these novel functions alone or as part of the R2TP complex [74].

Recent high-resolution studies of a co-crystal structure of a Pih1D1 and the Tel2 phosphopeptide, as well as several subcomplexes of the human and yeast R2TP complexes have started to address the structural bases of R2TP activity (Figure 7B) [75]. CryoEM and X-ray crystallography have also provided some insights into the structural organization of RuvBL1 and RuvBL2, which form the core of the R2TP (Figure 7C-7D) [76–79]. RuvBL1, also known as Pontin, and RuvBL2, also known as Reptin, are two conserved and closely related (65% sequence similarity) AAA+ ATP-ases homologous to prokaryotic RuvB [80]. The structures of human RuvBL1 and RuvBL2 are very similar, consisting of three distinct domains. Domain I (DI) and domain III (DIII) comprise the ATPase core that oligomerizes forming hexameric rings [78,79] (Figures 7B, panel iii and Figure 7C). Domain II (DII) is a unique insertion that connects directly to the ATPase core through a flexible region that permits the motion of DII. It has been shown that this domain is involved in protein-protein interactions as part of the INO80 and SWR1 remodelling

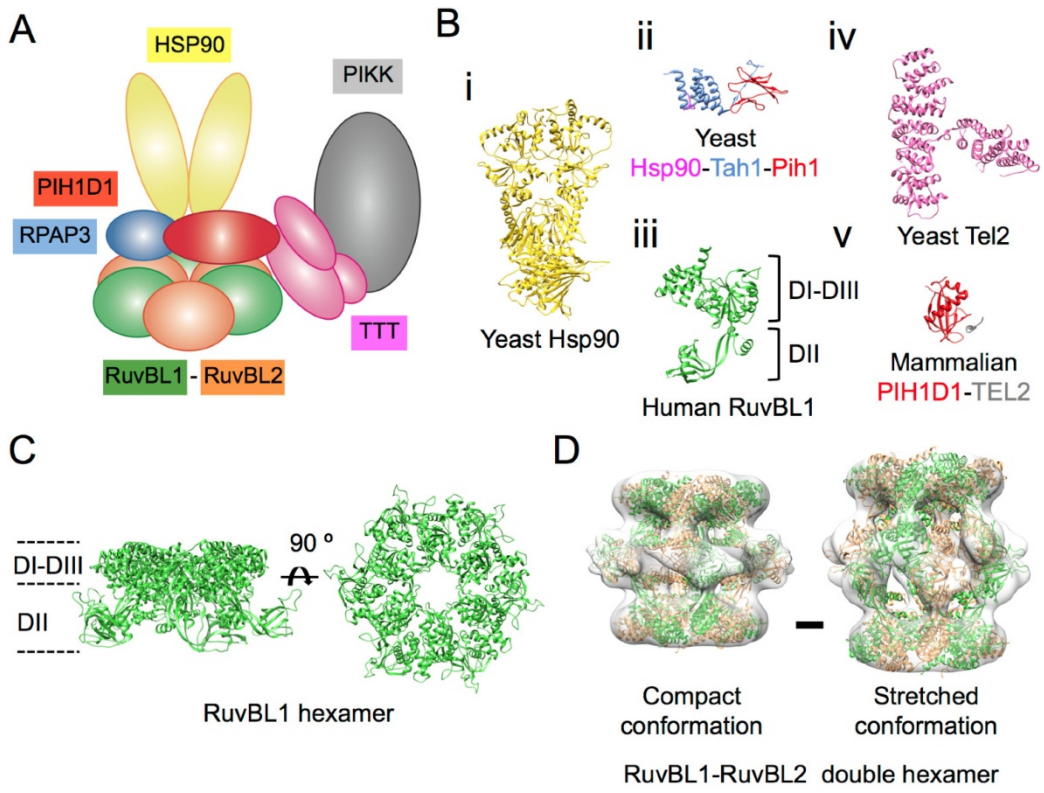

Figure 7. Assembly and maturation of PIKKs by RuvBL1-RuvBL2 and the R2TP complex. (A) Cartoon of the R2TP-HSP90 complex and its role in the maturation of PIKKs. The organization of the complex is unknown and thus, the cartoon is only based on the current information about the interactions within the complexes. (B) Ribbon representation of the atomic structures for some components of the PIKKs maturation machinery. (i) Full-length yeast Hsp90 (PDB numbered: 2CG9) [86]. (ii) Yeast Hsp90 peptide (in magenta) bound to Tah1-Pih1 (shown in blue and red respectively, PDB ID: 4CGU) [75]. (iii) Human RuvBL1 (PDB ID: 2C9O) [78]. Domains I, II and III are indicated. (iv) Yeast Tel2 (PDB ID: 3O4Z) [87]. (v) Mammalian PIH1D1 (in red) bound to a TEL2 phosphopeptide (in grey, PDB ID: 4CSE) [75]. (C) Two orthogonal views of the hexameric human RuvBL1 ring (PDB ID: 2C9O) [78]. Regions corresponding to domains I, II and III are indicated. (D) One view of the cryoEM structure of RuvBL1-RuvBL2 dodecamers in the compact (EMD-2163) and stretched (EMD-2164) conformations [77]. The EM structures are shown as a transparent density fitted with the atomic structures of a truncated dodecamer of human RuvBL1-RuvBL2 that lacks the DII domains of both proteins (PDB ID: 2XSZ) [79], and the DII domain of human RuvBL1 (from PDB ID: 2C9O) [78]. RuvBL1 is shown in green and RuvBL2 in light brown. The scale bar corresponds to 20 Å.

complexes [81,82]. RuvBL1 and RuvBL2 assemble into either homo or hetero-oligomeric hexamers, which can interact to form double-ring complexes [80,83]. CryoEM of double-ring complexes containing a roughly equimolar amount of human RuvBL1 and RuvBL2 revealed the co-existence of

two conformations within the same preparation, which were resolved by computational processing of single molecule images [77] (Figure 7D). It is yet not fully understood what the functional significance of each type oligomer *in vivo* is, and whether RuvBL1-RuvBL2 hexameric or dodecameric complexes or both are functionally relevant *in vivo*.

8. Future perspectives

Single-particle EM has been a major source of structural information for the PIKK family of kinases, due to their complex architecture and regulation. Nonetheless significant advances have only been possible thanks to the combination of the medium-low structural information obtained by EM, and also SAXS, and high-resolution data from crystallography. It is therefore expected that high-resolution EM structures, to be obtained thanks to direct electron detectors, will further contribute to our understanding of the mechanisms determining PIKK regulation in the fundamental cellular processes mediated by this family of kinases.

Acknowledgments

In this review, we attempted to cite original research articles as well as appropriate reviews and apologize for any unintentional omission of relevant publications. We want to acknowledge the contributions of Eva Torreira, Martín Alcorlo and Raquel Castaño, formers members of Llorca´s group, for their work on PIKKs and RuvBL1-RuvBL2. This work was supported by the "Ministerio de Economía y Competitividad", Spanish Government (grants SAF2011-22988 and SAF2014-52301-R to OL, and Juan de la Cierva contract JCI-2011-09536 to RM).

Conflict of Interest

All authors declare no conflicts of interest in this paper.

References

1. Baretic D, Williams RL (2014) PIKKs - the solenoid nest where partners and kinases meet. *Curr Opin Struct Biol* 29C: 134–142.
2. Lovejoy CA, Cortez D (2009) Common mechanisms of PIKK regulation. *DNA Repair (Amst)* 8: 1004–1008.
3. Lempiainen H, Halazonetis TD (2009) Emerging common themes in regulation of PIKKs and PI3Ks. *EMBO J* 28: 3067–3073.
4. van der Burg M, van Dongen JJ, van Gent DC (2009) DNA-PKcs deficiency in human: long predicted, finally found. *Curr Opin Allergy Clin Immunol* 9: 503–509.
5. Savitsky K, Bar-Shira A, Gilad S, et al. (1995) A single ataxia telangiectasia gene with a product similar to PI-3 kinase. *Science* 268: 1749–1753.
6. Weber AM, Ryan AJ (2014) ATM and ATR as therapeutic targets in cancer. *Pharmacol Ther*.
7. Roberts TL, Ho U, Luff J, et al. (2013) Smg1 haploinsufficiency predisposes to tumor formation and inflammation. *Proc Natl Acad Sci U S A* 110: E285–294.

8. Zoncu R, Efeyan A, Sabatini DM (2011) mTOR: from growth signal integration to cancer, diabetes and ageing. *Nat Rev Mol Cell Biol* 12: 21–35.
9. Kong X, Shen Y, Jiang N, et al. (2011) Emerging roles of DNA-PK besides DNA repair. *Cell Signal* 23: 1273–1280.
10. Kruger A, Ralser M (2011) ATM is a redox sensor linking genome stability and carbon metabolism. *Sci Signal* 4: pe17.
11. Oliveira V, Romanow WJ, Geisen C, et al. (2008) A protective role for the human SMG-1 kinase against tumor necrosis factor-alpha-induced apoptosis. *J Biol Chem* 283: 13174–13184.
12. Bosotti R, Isacchi A, Sonnhammer EL (2000) FAT: a novel domain in PIK-related kinases. *Trends Biochem Sci* 25: 225–227.
13. Keith CT, Schreiber SL (1995) PIK-related kinases: DNA repair, recombination, and cell cycle checkpoints. *Science* 270: 50–51.
14. Brewerton SC, Dore AS, Drake AC, et al. (2004) Structural analysis of DNA-PKcs: modelling of the repeat units and insights into the detailed molecular architecture. *J Struct Biol* 145: 295–306.
15. Perry J, Kleckner N (2003) The ATRs, ATMs, and TORs are giant HEAT repeat proteins. *Cell* 112: 151–155.
16. Sommer LA, Schaad M, Dames SA (2013) NMR- and circular dichroism-monitored lipid binding studies suggest a general role for the FATC domain as membrane anchor of phosphatidylinositol 3-kinase-related kinases (PIKK). *J Biol Chem* 288: 20046–20063.
17. Lucero H, Gae D, Taccioli GE (2003) Novel localization of the DNA-PK complex in lipid rafts: a putative role in the signal transduction pathway of the ionizing radiation response. *J Biol Chem* 278: 22136–22143.
18. Dames SA (2010) Structural basis for the association of the redox-sensitive target of rapamycin FATC domain with membrane-mimetic micelles. *J Biol Chem* 285: 7766–7775.
19. Sancak Y, Bar-Peled L, Zoncu R, et al. (2010) Ragulator-Rag complex targets mTORC1 to the lysosomal surface and is necessary for its activation by amino acids. *Cell* 141: 290–303.
20. Morita T, Yamashita A, Kashima I, et al. (2007) Distant N- and C-terminal domains are required for intrinsic kinase activity of SMG-1, a critical component of nonsense-mediated mRNA decay. *J Biol Chem* 282: 7799–7808.
21. Yang H, Rudge DG, Koos JD, et al. (2013) mTOR kinase structure, mechanism and regulation. *Nature* 497: 217–223.
22. Sirbu BM, Cortez D (2013) DNA damage response: three levels of DNA repair regulation. *Cold Spring Harb Perspect Biol* 5: a012724.
23. Ochi T, Wu Q, Blundell TL (2014) The spatial organization of non-homologous end joining: from bridging to end joining. *DNA Repair (Amst)* 17: 98–109.
24. Spagnolo L, Rivera-Calzada A, Pearl LH, et al. (2006) Three-dimensional structure of the human DNA-PKcs/Ku70/Ku80 complex assembled on DNA and its implications for DNA DSB repair. *Mol Cell* 22: 511–519.
25. Hammel M, Yu Y, Mahaney BL, et al. (2010) Ku and DNA-dependent protein kinase dynamic conformations and assembly regulate DNA binding and the initial non-homologous end joining complex. *J Biol Chem* 285: 1414–1423.
26. Lee JH, Paull TT (2005) ATM activation by DNA double-strand breaks through the Mre11-Rad50-Nbs1 complex. *Science* 308: 551–554.

27. Zou L, Elledge SJ (2003) Sensing DNA damage through ATRIP recognition of RPA-ssDNA complexes. *Science* 300: 1542–1548.
28. Heitman J, Movva NR, Hall MN (1991) Targets for cell cycle arrest by the immunosuppressant rapamycin in yeast. *Science* 253: 905–909.
29. Laplante M, Sabatini DM (2012) mTOR signaling in growth control and disease. *Cell* 149: 274–293.
30. Shimobayashi M, Hall MN (2014) Making new contacts: the mTOR network in metabolism and signalling crosstalk. *Nat Rev Mol Cell Biol* 15: 155–162.
31. Yamashita A (2013) Role of SMG-1-mediated Upf1 phosphorylation in mammalian nonsense-mediated mRNA decay. *Genes Cells* 18: 161–175.
32. Yamashita A, Izumi N, Kashima I, et al. (2009) SMG-8 and SMG-9, two novel subunits of the SMG-1 complex, regulate remodeling of the mRNA surveillance complex during nonsense-mediated mRNA decay. *Genes Dev* 23: 1091–1105.
33. Ivanov PV, Gehring NH, Kunz JB, et al. (2008) Interactions between UPF1, eRFs, PABP and the exon junction complex suggest an integrated model for mammalian NMD pathways. *Embo J* 27: 736–747.
34. Kashima I, Yamashita A, Izumi N, et al. (2006) Binding of a novel SMG-1-Upf1-eRF1-eRF3 complex (SURF) to the exon junction complex triggers Upf1 phosphorylation and nonsense-mediated mRNA decay. *Genes Dev* 20: 355–367.
35. Murr R, Vaissiere T, Sawan C, et al. (2007) Orchestration of chromatin-based processes: mind the TRRAP. *Oncogene* 26: 5358–5372.
36. McMahon SB, Wood MA, Cole MD (2000) The essential cofactor TRRAP recruits the histone acetyltransferase hGCN5 to c-Myc. *Mol Cell Biol* 20: 556–562.
37. Sibanda BL, Chirgadze DY, Blundell TL (2010) Crystal structure of DNA-PKcs reveals a large open-ring cradle comprised of HEAT repeats. *Nature* 463: 118–121.
38. Stark H (2010) GraFix: stabilization of fragile macromolecular complexes for single particle cryo-EM. *Methods Enzymol* 481: 109–126.
39. Boskovic J, Rivera-Calzada A, Maman JD, et al. (2003) Visualization of DNA-induced conformational changes in the DNA repair kinase DNA-PKcs. *EMBO J* 22: 5875–5882.
40. Melero R, Uchiyama A, Castano R, et al. (2014) Structures of SMG1-UPFs complexes: SMG1 contributes to regulate UPF2-dependent activation of UPF1 in NMD. *Structure* 22: 1105–1119.
41. Dames SA, Mulet JM, Rathgeb-Szabo K, et al. (2005) The solution structure of the FATC domain of the protein kinase target of rapamycin suggests a role for redox-dependent structural and cellular stability. *J Biol Chem* 280: 20558–20564.
42. Leone M, Crowell KJ, Chen J, et al. (2006) The FRB domain of mTOR: NMR solution structure and inhibitor design. *Biochemistry* 45: 10294–10302.
43. Yip CK, Murata K, Walz T, et al. (2010) Structure of the human mTOR complex I and its implications for rapamycin inhibition. *Mol Cell* 38: 768–774.
44. Williams DR, Lee KJ, Shi J, et al. (2008) Cryo-EM structure of the DNA-dependent protein kinase catalytic subunit at subnanometer resolution reveals alpha helices and insight into DNA binding. *Structure* 16: 468–477.
45. Rivera-Calzada A, Maman JD, Spagnolo L, et al. (2005) Three-dimensional structure and regulation of the DNA-dependent protein kinase catalytic subunit (DNA-PKcs). *Structure* 13: 243–255.

46. Kuhlbrandt W (2014) Cryo-EM enters a new era. *Elife* 3: e03678.
47. Llorca O, Rivera-Calzada A, Grantham J, et al. (2003) Electron microscopy and 3D reconstructions reveal that human ATM kinase uses an arm-like domain to clamp around double-stranded DNA. *Oncogene* 22: 3867–3874.
48. Arias-Palomo E, Yamashita A, Fernandez IS, et al. (2011) The nonsense-mediated mRNA decay SMG-1 kinase is regulated by large-scale conformational changes controlled by SMG-8. *Genes Dev* 25: 153–164.
49. Adami A, Garcia-Alvarez B, Arias-Palomo E, et al. (2007) Structure of TOR and its complex with KOG1. *Mol Cell* 27: 509–516.
50. Chiu CY, Cary RB, Chen DJ, et al. (1998) Cryo-EM imaging of the catalytic subunit of the DNA-dependent protein kinase. *J Mol Biol* 284: 1075–1081.
51. Leuther KK, Hammarsten O, Kornberg RD, et al. (1999) Structure of DNA-dependent protein kinase: implications for its regulation by DNA. *EMBO J* 18: 1114–1123.
52. Grinthal A, Adamovic I, Weiner B, et al. (2010) PR65, the HEAT-repeat scaffold of phosphatase PP2A, is an elastic connector that links force and catalysis. *Proc Natl Acad Sci USA* 107: 2467–2472.
53. Forwood JK, Lange A, Zachariae U, et al. (2010) Quantitative structural analysis of importin-beta flexibility: paradigm for solenoid protein structures. *Structure* 18: 1171–1183.
54. Knutson BA (2010) Insights into the domain and repeat architecture of target of rapamycin. *J Struct Biol* 170: 354–363.
55. Spagnolo L, Barbeau J, Curtin NJ, et al. (2012) Visualization of a DNA-PK/PARP1 complex. *Nucleic Acids Res* 40: 4168–4177.
56. Morris EP, Rivera-Calzada A, da Fonseca PC, et al. (2011) Evidence for a remodelling of DNA-PK upon autophosphorylation from electron microscopy studies. *Nucleic Acids Res* 39: 5757–5767.
57. Bakkenist CJ, Kastan MB (2003) DNA damage activates ATM through intermolecular autophosphorylation and dimer dissociation. *Nature* 421: 499–506.
58. Perry JJ, Tainer JA (2011) All stressed out without ATM kinase. *Sci Signal* 4: pe18.
59. Guo Z, Kozlov S, Lavin MF, et al. (2010) ATM activation by oxidative stress. *Science* 330: 517–521.
60. Shiloh Y, Ziv Y (2013) The ATM protein kinase: regulating the cellular response to genotoxic stress, and more. *Nat Rev Mol Cell Biol* 14: 197–210.
61. Dynan WS, Yoo S (1998) Interaction of Ku protein and DNA-dependent protein kinase catalytic subunit with nucleic acids. *Nucleic Acids Res* 26: 1551–1559.
62. Neal JA, Sugiman-Marangos S, VanderVere-Carozza P, et al. (2014) Unraveling the complexities of DNA-dependent protein kinase autophosphorylation. *Mol Cell Biol* 34: 2162–2175.
63. Meek K, Douglas P, Cui X, et al. (2007) trans Autophosphorylation at DNA-dependent protein kinase's two major autophosphorylation site clusters facilitates end processing but not end joining. *Mol Cell Biol* 27: 3881–3890.
64. Dobbs TA, Tainer JA, Lees-Miller SP (2010) A structural model for regulation of NHEJ by DNA-PKcs autophosphorylation. *DNA Repair (Amst)* 9: 1307–1314.
65. Villarreal SA, Stewart PL (2014) CryoEM and image sorting for flexible protein/DNA complexes. *J Struct Biol* 187: 76–83.

66. Wu PY, Ruhlmann C, Winston F, et al. (2004) Molecular architecture of the S. cerevisiae SAGA complex. *Mol Cell* 15: 199–208.
67. Chittuluru JR, Chaban Y, Monnet-Saksouk J, et al. (2011) Structure and nucleosome interaction of the yeast NuA4 and Piccolo-NuA4 histone acetyltransferase complexes. *Nat Struct Mol Biol* 18: 1196–1203.
68. Kozlov SV, Graham ME, Jakob B, et al. (2011) Autophosphorylation and ATM activation: additional sites add to the complexity. *J Biol Chem* 286: 9107–9119.
69. Zhao R, Davey M, Hsu YC, et al. (2005) Navigating the chaperone network: an integrative map of physical and genetic interactions mediated by the hsp90 chaperone. *Cell* 120: 715–727.
70. Boulon S, Bertrand E, Pradet-Balade B (2012) HSP90 and the R2TP co-chaperone complex: building multi-protein machineries essential for cell growth and gene expression. *RNA Biol* 9: 148–154.
71. Hurov KE, Cotta-Ramusino C, Elledge SJ (2010) A genetic screen identifies the Triple T complex required for DNA damage signaling and ATM and ATR stability. *Genes Dev* 24: 1939–1950.
72. Takai H, Wang RC, Takai KK, et al. (2007) Tel2 regulates the stability of PI3K-related protein kinases. *Cell* 131: 1248–1259.
73. Horejsi Z, Takai H, Adelman CA, et al. (2010) CK2 phospho-dependent binding of R2TP complex to TEL2 is essential for mTOR and SMG1 stability. *Mol Cell* 39: 839–850.
74. Izumi N, Yamashita A, Iwamatsu A, et al. (2010) AAA+ proteins RUVBL1 and RUVBL2 coordinate PIKK activity and function in nonsense-mediated mRNA decay. *Sci Signal* 3: ra27.
75. Pal M, Morgan M, Phelps SE, et al. (2014) Structural basis for phosphorylation-dependent recruitment of Tel2 to Hsp90 by Pih1. *Structure* 22: 805–818.
76. Torreira E, Jha S, Lopez-Blanco JR, et al. (2008) Architecture of the pontin/reptin complex, essential in the assembly of several macromolecular complexes. *Structure* 16: 1511–1520.
77. Lopez-Perrote A, Munoz-Hernandez H, Gil D, et al. (2012) Conformational transitions regulate the exposure of a DNA-binding domain in the RuvBL1-RuvBL2 complex. *Nucleic Acids Res* 40: 11086–11099.
78. Matias PM, Gorynia S, Donner P, et al. (2006) Crystal structure of the human AAA+ protein RuvBL1. *J Biol Chem* 281: 38918–38929.
79. Gorynia S, Bandeiras TM, Pinho FG, et al. (2011) Structural and functional insights into a dodecameric molecular machine - the RuvBL1/RuvBL2 complex. *J Struct Biol* 176: 279–291.
80. Huen J, Kakihara Y, Ugwu F, et al. (2010) Rvb1-Rvb2: essential ATP-dependent helicases for critical complexes. *Biochem Cell Biol* 88: 29–40.
81. Tosi A, Haas C, Herzog F, et al. (2013) Structure and subunit topology of the INO80 chromatin remodeler and its nucleosome complex. *Cell* 154: 1207–1219.
82. Nguyen VQ, Ranjan A, Stengel F, et al. (2013) Molecular architecture of the ATP-dependent chromatin-remodeling complex SWR1. *Cell* 154: 1220–1231.
83. Jha S, Dutta A (2009) RVB1/RVB2: running rings around molecular biology. *Mol Cell* 34: 521–533.
84. Melero R, Buchwald G, Castano R, et al. (2012) The cryo-EM structure of the UPF-EJC complex shows UPF1 poised toward the RNA 3' end. *Nat Struct Mol Biol* 19: 498–505, S491–492.
85. Chakrabarti S, Jayachandran U, Bonneau F, et al. (2011) Molecular mechanisms for the RNA-dependent ATPase activity of Upf1 and its regulation by Upf2. *Mol Cell* 41: 693–703.

86. Ali MM, Roe SM, Vaughan CK, et al. (2006) Crystal structure of an Hsp90-nucleotide-p23/Sba1 closed chaperone complex. *Nature* 440: 1013–1017.
87. Takai H, Xie Y, de Lange T, et al. (2010) Tel2 structure and function in the Hsp90-dependent maturation of mTOR and ATR complexes. *Genes Dev* 24: 2019–2030.